International Journal of Lightweight Materials and Manufacture 5 (2022) 520–527

Contents lists available at ScienceDirect

International Journal of Lightweight Materials and Manufacture

journal homepage: www.keaipublishing.com/ijlmm

Fabrication of light-weighted acoustic absorbers made of natural fiber composites via additive manufacturing

Vignesh Sekar [a, *], Se Yong Eh Noum [a], Azma Putra [b], Sivakumar Sivanesan [c], Desmond Daniel Chin Vui Sheng [d]

[a] School of Computer Science and Engineering, Taylor's University, 47500, Subang Jaya, Selangor, Malaysia
[b] Centre for Advanced Research on Energy, Universiti Teknikal Malaysia Melaka (UTeM), Melaka, Malaysia
[c] School of Engineering, Asia Pacific University, Kuala Lumpur, Malaysia
[d] Applied Mechanics Research and Consultancy Group (AMRCG), School of Mechanical Engineering, Faculty of Engineering, Universiti Teknologi Malaysia, 81310 Skudai, Johor Bahru, Malaysia

ARTICLE INFO

Article history:
Received 5 April 2022
Received in revised form
21 June 2022
Accepted 22 June 2022
Available online 28 June 2022

Keywords:
Light-weighted sound absorbers
Additive manufacturing
Acoustics
Natural fiber composites
Two microphone impedance tube method

ABSTRACT

Synthetic fiber is still considered the best sound absorptive material. However, due to the health concern of synthetic fiber usage, researchers are trying to find another viable alternative. A microperforated panel (MPP) is a promising alternative that relies on the concept of a Helmholtz resonator for sound absorption. MPP possessed excellent acoustic resistance and a considerable range of absorption bandwidth. In this paper, MPP made of natural fiber composite was fabricated and its acoustic absorption was measured using a two-microphone impedance tube method as per ISO 10534-2 standard. Later, the tensile strength of the fabricated acoustic absorbers was measured using an Instron Universal Testing Machine as per ASTM D638. The idea of employing additive manufacturing, better known as the 3D printing technique, is proposed to produce lightweight MPP. The 3D printing technique provides design freedom and is less tedious in creating complex and light structures. The 3D printing technique has various important parameters, and infill density is one of the parameters. It was found that the reduction of infill density leads to a decrease of the MPP's mass and thus, slightly affects the resonance frequency of the MPP, still within the mid-frequency spectrum. It was also noted that the increment of air gap thickness leads to the shifting of MPP's resonance frequency to a lower frequency range. The tensile strength of the 3D printed samples decreases with a decrease in infill density. A sample with an infill density of 100% has the highest tensile strength of 22 MPa, and a sample with an infill density of 20% has the lowest tensile strength of 12 MPa.

1. Introduction

In this era of globalization and modernization, the noise level gradually gets louder in an uncontrolled manner. As a result, people realized that noise could affect a person psychologically and physiologically. Prolonged noise exposure may cause stress elevation, temper tolerance reduction, intractable sleeping problems, and, if worse, might lead to irreparable hearing complications [1]. A lot of methods can be employed for noise control. The most popular way is to install an acoustic absorber to solve the acoustic problem within a designated space or room, as it is the most practical and economical approach. There are mainly two types of acoustic absorbers; they are porous absorbers and resonant absorbers [2]. Porous absorbers are solid materials that contain cavities, channels, or interstices to provide a path for sound waves. These materials include fiberboard, rock wool, foams, and natural fibers connected to pores where the sound waves spread [3]. Resonance absorbers are further classified into membrane and Helmholtz absorbers. Perforated panels which are considered as good example of Helmholtz absorbers acts as a viable alternative to improve a built environment's acoustic condition in recent times [4]. It can be installed as a wall partition, window, fluorescent light overlay, sunshade, or column cover [5]. The perforated panel possesses

* Corresponding author.
E-mail address: svikiviki94@gmail.com (V. Sekar).
Peer review under responsibility of Editorial Board of International Journal of Lightweight Materials and Manufacture.

https://doi.org/10.1016/j.ijlmm.2022.06.007

reasonable sound absorption capability at medium frequency range or higher but exhibits poor sound absorption capability at lower frequency range [6].

In 1975, Professor Dah You Maa proposed a microperforated panel (MPP) for sound absorption purposes [7]. MPP is a particularly thin panel that comprises a substantial amount of microperforated holes [8]. The perforated hole's diameter and the panel thickness are commonly less than 1 mm. The sum of microperforated holes is usually between 1% and 2% of the panel's total surface area [9]. An air space must be introduced between MPP and a fixed wall to absorb sound effectively. MPP depends greatly on the air particle wigwag motion around the microperforated holes to absorb sound. The friction between the air particles and the inner surface of microperforated holes causes deterioration of sound energy by converting it to heat and thus, absorbing sound [10]. It has been found that MPP possessed significantly higher acoustic resistance and a much wider bandwidth of absorption than the perforated panel, even without the inclusion of porous material [11]. Fig. 1 illustrates the sound absorption mechanism of MPP.

MPP exhibits elegant and attractive appearance as it can be made from various materials such as acrylic glass, plywood, metal, and plastic suitable for interior architectural purposes [13]. For instance, a MPP made from acrylic glass can absorb sound excellently without blocking and hindering light rays from passing through it [14]. It has been proven that fiberglass and rock wool exhibit excellent sound absorption characteristics [15]. Yet, prolonged exposure to these synthetic materials is deleterious to our health. Synthetic fibers are often made from petrochemical resources and require high temperatures for the manufacturing process, which may negatively contribute to the hikes in carbon footprint [16]. Polymers like polylactic acid (PLA) and polyhydroxyalkanoates (PHA) have received a lot of attention in recent years because of their biodegradability and made from renewable resources [17]. Wood fiber (WF) based acoustic absorbers have become the famous choice for acousticians since wood-based acoustic absorbers are aesthetically good and exhibit better acoustic absorption [18]. Wood is recyclable, reusable, renewable, and has a high sustainability rate. Furthermore, its excellent strength-to-weight ratios, thermally insulating, and acoustical properties make it suitable for a wide range of building applications, including structural beams and frames, insulating envelopes, windows, door frames, wall and flooring materials, and furniture [19].

Inorganic soundproof panels are commonly used in the field of building sound insulation, particularly in cement and concrete. These inorganic materials have high surface density, high strength, and good insulation, in addition to good weathering resistance. However, it has issues with its heavy weight [20]. In recent times, additive manufacturing (or) 3D printing has already rooted its application into the field of acoustics and has the advantage with the freedom of design and the ability to build complex and lightweight structures [21]. Additive manufacturing process has variety of process parameters. Infill density, which is defined as the amount of filament used in printing the structure, is one of the parameters. It is usually expressed as a percentage and ranges from 10% to 100%. Printed structures with a 10% infill density will be hollow, and the infill density will increase as the material consumption increases. Printed structures with 100% infill density are more solid. Vignesh et al. demonstrated the effect of infill density on acoustic absorption of the porous absorber (absorber without perforations), whereas the effect of infill density on acoustic absorption of the perforated absorber was presented in this study [22]. Noises come from different sources falls under different spectrums. The spectrums may be of mainly low, mid and high-frequency [23]. These noises that comes from various spectrums are difficult to control with a single absorber because it comes in a variety of spectrums. Considering all the above stated problems, this research aims to fabricate the light-weighted acoustic absorbers made of natural fiber composites by reducing the infill density in the additive manufacturing process and to absorb sound at various spectrum by altering the air gap.

2. Theory of MPP

Maa proposed a theoretical model that can be used to predict the sound absorption of MPP simply by considering the microperforated hole as a narrow circular tube, as shown in Fig. 2. If the

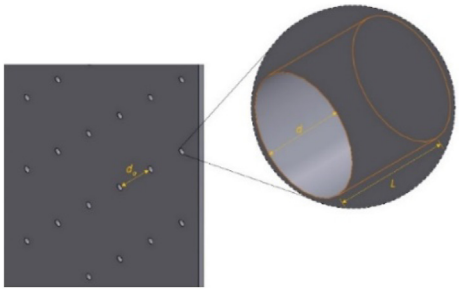

Fig. 2. The microperforated hole depicted as a narrow circular tube.

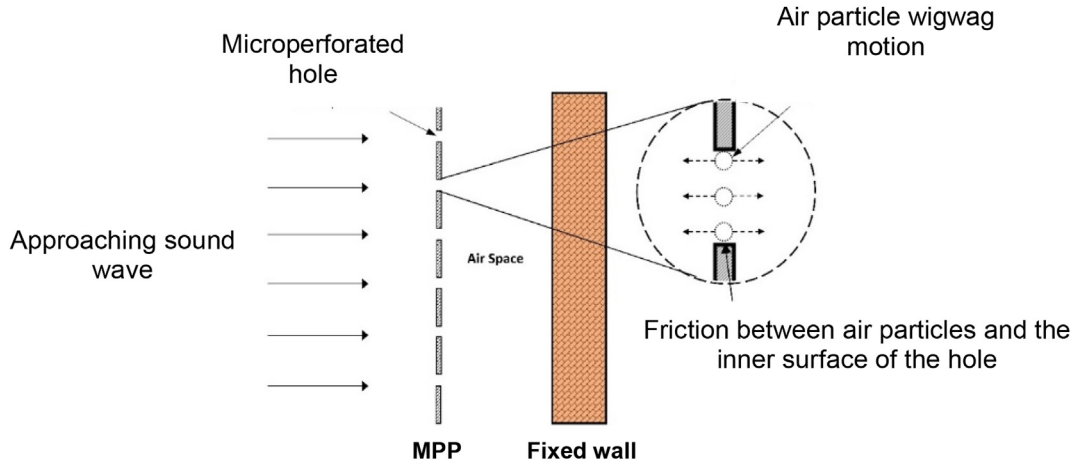

Fig. 1. Sound absorption mechanism of MPP [12].

wavelength of the incident sound wave is more significant than both the diameter (d) and the distance between the adjacent tubes (d_a), the tube's acoustic impedance (Z) can be formulated as [24]:

$$Z = \frac{j\omega\rho L}{1 - \left(\frac{J_1}{J_0}\right)\left(2r\frac{\sqrt{-j}}{\sqrt{-j}}\left(\frac{\eta}{\rho\omega}\right)\right)\left(\frac{\rho\omega}{r\eta\sqrt{-j}}\right)} \quad (1)$$

$$\omega = 2\pi f \quad (2)$$

where ω, ρ, L, r, and η are defined as sound angular frequency, air density, length of the tube (MPP thickness), a radius of tube (microperforated hole radius), and air dynamic viscosity respectively, while J_0 and J_1 are defined as the zeroth and first-order Bessel functions of the first kind respectively. To compute the acoustic impedance of MPP, Eq. (1) must be divided by the ratio of microperforated area. However, Eq. (1) required tedious computation and calculation process and has been deemed as inconvenient and impractical. Thus, Maa suggested another better equation with a marginal error of less than 5%, and the normalized acoustic impedance of MPP (Z_n) can be formulated as [7]:

$$Z_n = R_n + jX_n \quad (3)$$

$$R_n = \left(\frac{d_0\chi\sqrt{2}}{8L} + \sqrt{\frac{\chi^2}{32} + 1}\right) \times \frac{B_1 L}{p{d_0}^2} \times 10^{-5} \quad (4)$$

$$X_n = \left(\frac{1}{\sqrt{\frac{\chi^2}{2} + 9}} + \frac{0.85d_0}{L} + 1\right) \times \frac{fL}{p} \times 0.0185 \quad (5)$$

$$\chi = B_2 d_0 \sqrt{f} \times 10^{-3} \quad (6)$$

where R_n and X_n are defined as the resistance and reactance of MPP, respectively. f, p, and d_0 are defined as the frequency of approaching sound wave, a ratio of microperforated area, and the diameter of a microperforated hole, respectively. B_1 and B_2 are defined as constants for the normalized equation. Table 1 shows the constant value for B_1 and B_2 for metallic and non-metallic MPP.

Finally, the sound absorption coefficient of MPP (α) under normal incidence condition backed by an air space can be expressed as [25]:

$$\alpha = \frac{4R_n}{(R_n + 1)^2 + \left(X_n\omega - \cot\left(\frac{\omega D}{c}\right)\right)^2} \quad (7)$$

where c is defined as the speed of approaching sound waves.

Table 1
Constant value for B_1 and B_2.

Constant	Value	
	Metallic	Non-metallic
B_1	0.335	0.147
B_2	0.210	0.316

3. Experimental

3.1. Materials

Polylactic acid/polyhydroxyalkanoates-wood fibers (PLA/PHA-WF) composite was commercially available in the form of filament and hence outsourced from ColorFabb, DK Belfeld, Netherlands under the trade name woodfill. The filament has a standard diameter of 1.75 ± 0.05 mm, and the density of the filament is 1.15 g/cm^3 with a melting temperature of greater than 155 °C.

3.2. Methodology

Raise 3D N2 Plus printer was used to 3D print the MPP. It prints the MPP layer by layer using fused deposition modelling technology. MPP are 3D printed at a rate of 70 mm/s at a melting temperature of 210 °C. These values were chosen from the recommended datasheet provided by ColorFabb. MPP were 3D printed for a thickness of 5 mm with varying infill densities (100%, 80%, 60%, 40%, 20%). The layers which show the difference in infill density are printed between the normally printed layers as shown in Fig. 3. The perforation diameter was 0.6 mm with a 5 mm distance between the perforations. The perforation diameter and the distance between the perforations were adopted from Liu et al. for better acoustic resistance [26]. Few cloggages were seen inside the perforations and the cloggages inside the perforations were cleared using a needle of 0.6 mm.

3.3. Characterization of MPP

3.3.1. Mass

3D printed MPP (3DP-MPP) were weighed using a top-loading balance machine with a repeatability of 0.001 g.

3.3.2. Density

The density of the successfully developed MPP was measured using the Mettler Toledo ME204 density meter referring to the ASTM D792 testing standard. The measurement of density works on the Archimedes immersion technique. The density (in g/cm^3) of the MPP was obtained experimentally using the results of two measurements, i.e. mass of sample in the air and mass of the sample in distilled water at 25 ± 2 °C with the relative humidity of 65 ± 5%. The density of the MPP was calculated experimentally as per Eq. (9).

$$\textit{Density of MPP} = \frac{u}{u - v} \times \textit{Density of water} \quad (9)$$

where u is the mass of sample in the air (in g), v is the mass of sample immersed in water (in g). Table 2 shows the specification of the MPP samples.

3.3.3. Acoustic absorption

Sound absorption coefficient (SAC) was measured by using a two microphone impedance tube method as per ISO 10534-2 standard [27]. The tube's inner diameter is 33.4 mm which is the diameter of the sample, and the outer diameter of the tube is 55 mm. Results are provided in the frequency range of 500 Hz to 4.5 kHz which is the valid frequency range considering the distance of the microphones and the diameter of the tube. First, SAC was measured for the MPP with varying infill densities. Next, SAC was measured for the 3D-MPP-100 with varying air gap. Prior to the experiment, the microphones were calibrated with a sound calibrator to ensure that the sound pressure inside the tube was accurately measured. To ensure repeatability, the measurement was repeated three times. For each measurement, the sample was removed and reinserted into the sample holder, and the variability

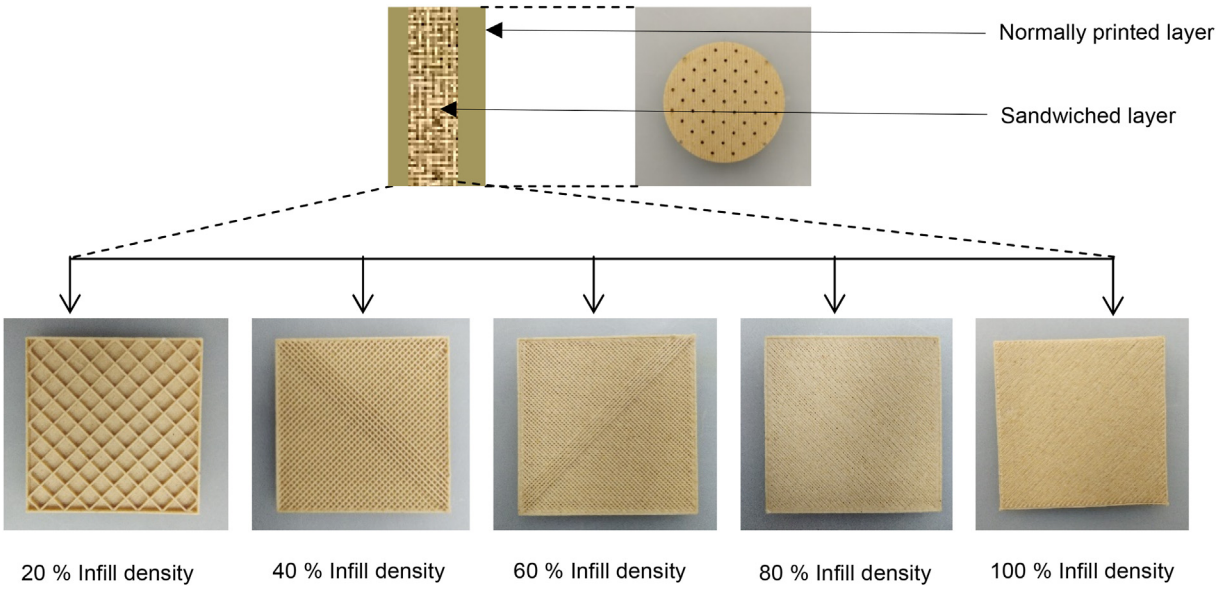

Fig. 3. 3D printed MPP with different infill density.

Table 2
Specification of the MPP samples.

Sample ID	Thickness (mm)	Infill Density (%)	Mas (g)	Density (g/cm^3)
3DP-MPP-100 (Control)	5.00	100.00	4.03	0.94
3DP-MPP-80	5.00	80.00	3.64	0.84
3DP-MPP-60	5.00	60.00	3.21	0.74
3DP-MPP-40	5.00	40.00	2.78	0.64
3DP-MPP-20	5.00	20.00	2.33	0.54

was found to be negligible for all samples. Fig. 4 shows the acoustic testing used in this study.

3.3.4. Tensile strength

Mechanical strength of the material can determine the quality of the final product. Hence, the tensile strength of the fabricated absorbers with varying infill densities was tested. Three dog-bone samples at each infill densities were 3D printed, tested for its tensile strength and its average value along with its standard deviations were reported and discussed. The tensile testing conditions and specifications were chosen in accordance with ASTM D638. Tensile strength was determined for the dog-bone samples using an Instron Universal Testing Machine (load cell of 50 kN) at a speed of 20 mm/min.

4. Results and discussion

4.1. Comparison of predicted and measured results

Fig. 5 compares the predicted and measured SAC of the control sample, 3DP-MPP-100 backed by an air gap of 5 mm. Predicted results are obtained from the MAA model. The maximum peak of

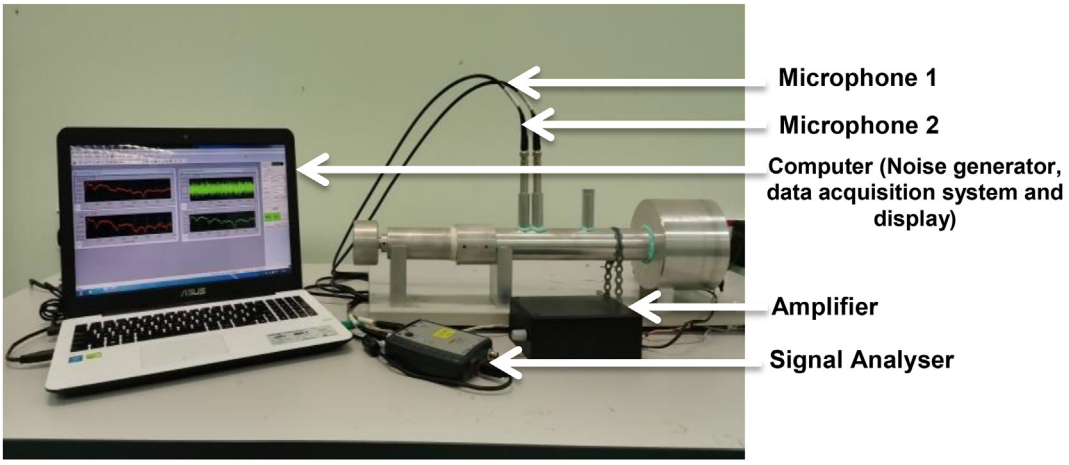

Fig. 4. Acoustic testing setup.

acoustic absorption recorded was 0.9 at a resonance frequency of 2.07 kHz. The measured results show a closer trend to predicted results with a minor deviation. The deviation between the predicted and measured results can be due to: (i) the procedure followed during the installation of the sample and its mounting condition [28]; (ii) the effect of eigenmode vibration happened in the mass-spring setup of the panel [29].

4.2. Effect of density on SAC

In the case of density, it can be seen from Table 2 that the density of the 3D printed samples tends to decrease with a decrease in infill density. MPP printed with 100% infill density was more solid and dense. The filament amount used to print a sample with an infill density of 100% was more compared to sample with 20% infill density was less. The mass of the MPP with 100%–20% infill density was reduced from 4.03 g to 2.33 g. The difference in material consumption varies the mass, which in turn alters the densities of the samples with different infill densities. The printed sample density with an infill density of 100% was 0.94 g/cm^3, and the density of the printed sample with an infill density of 20% was 0.54 g/cm^3. Fig. 6 shows the effect of infill density on SAC of the 3D printed MPP. It can be seen from Fig. 6 that the MPP with varying densities exhibits a narrow peak of acoustic absorption at mid-frequency spectrum which is a typical characteristic of the MPP. The maximum SAC of MPP for all densities were almost similar which was greater than 0.9. Varying densities to the MPP slightly affect the resonant frequencies of the MPP which was previously reported by the other researchers [30,31]. It can be seen from Fig. 6 that there is a slight movement of resonant frequency towards the high-frequency spectrum as the density decreases. The reduction in density caused a decrease in performance at low frequency as wave propagation became loose to the material, and thus absorption took effect on the shorter wavelength at higher frequency. However, the range of resonant frequencies for MPP with 100%–20% infill density was between 2000 Hz and 2600 Hz which was still within the mid-frequency spectrum. Hence, it can be inferred that the reduction in infill density reduces the mass of the MPP and slightly affects the resonant frequency of the MPP but the range falls within the mid-frequency spectrum.

4.3. Effect of an air gap on SAC

Fig. 7 shows the effect of air gap on the SAC of the 3DP-MPP-100. It can be seen from Fig. 7 that there was no peak of acoustic absorption for the case without an air gap. The mass (perforated end) and spring (air gap) system is the reason for resonant peaks and without an air gap, there will not be the formation of this system, which leads to the absence of resonant peaks. It can also be seen from Fig. 7 that the peak of sound absorption gets shifted towards the low-frequency spectrum as the air gap thickness increases. The following phenomena can explain the above trends; the perforated end acts as an acoustic mass, while the air occupying the tube within this space acts as an acoustic spring. These both replicate the mass-spring relation, and as the thickness of the air gap increases, the stiffness amid it decreases, thus shifting the peaks of sound absorption towards the low-frequency spectrum. Once the sound's frequency matches the resonance frequency, the stiffness of the air gap cancels the acoustic mass, which in turn causes the peaks of sound absorption to happen. 3D printed MPP with an infill density of 100% at an air gap of 15 mm shows the maximum SAC of almost unity at 1100 Hz.

4.4. Effect of density on tensile strength

Fig. 8 shows the effect of varying densities on the tensile strength of the fabricated acoustic absorbers. It can be seen from Fig. 8 that the tensile strength of the acoustic absorbers decreases with a decrease in infill densities. A sample with an infill density of 100% has the highest tensile strength of 22 MPa and a sample with

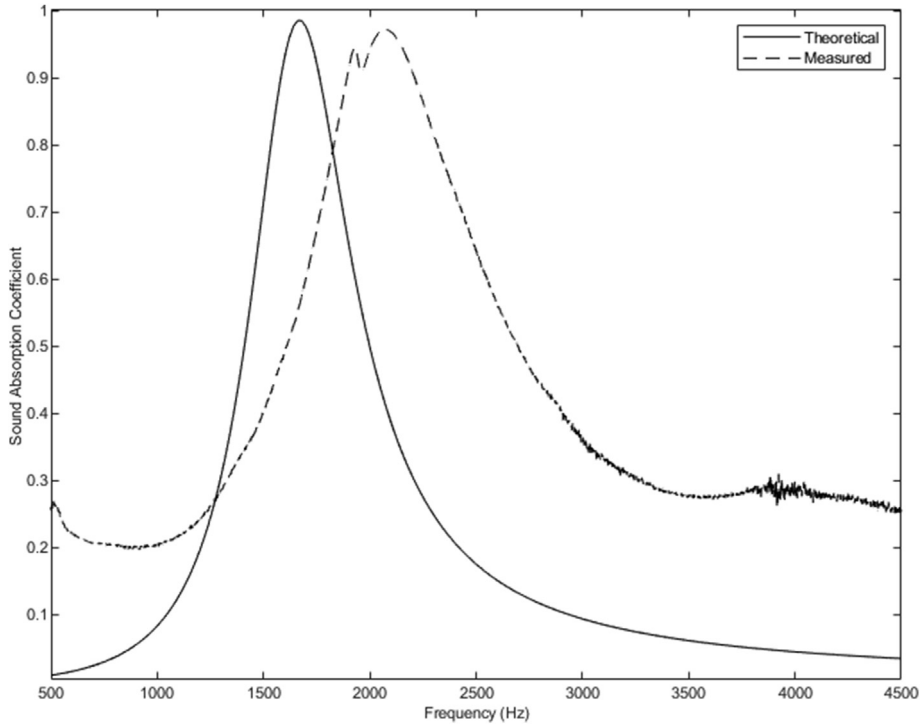

Fig. 5. Predicted and measured SAC of 3DP-MPP-100 backed by an air gap of 5 mm.

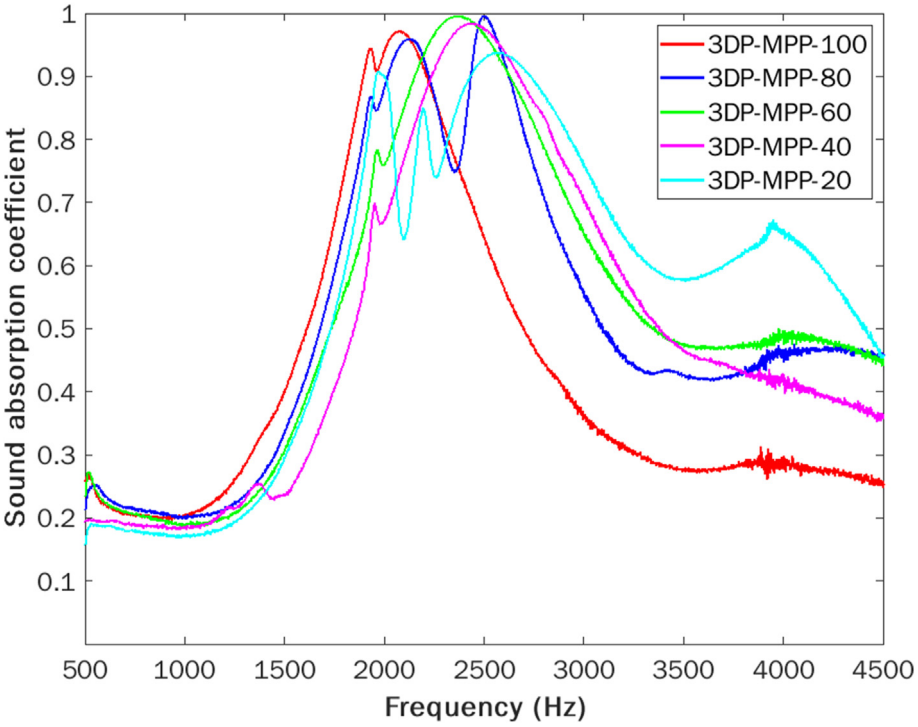

Fig. 6. Measured SAC of 3DP-MPP at varying infill densities backed by an air gap of 5 mm.

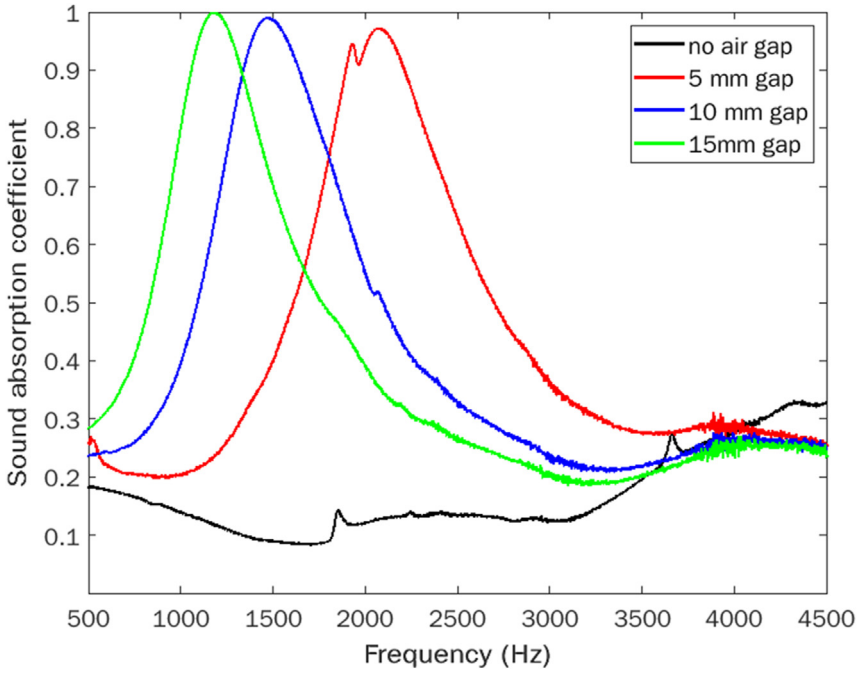

Fig. 7. Measured SAC of 3DP-MPP-100 at varying air gap thickness.

an infill density of 20% has the lowest tensile strength of 12 MPa. The difference in infill densities has caused the variation in the tensile strength of the samples. For the sample 3D printed with 100% infill density, the voids inside the structure were lesser, and subsequently increased tensile strength compared to the sample 3D printed with 20% infill density.

As shown in Fig. 9, the voids inside the structures for 100% infill density and 20% infill density can be visible at the region of fracture. The voids in the 3D printed structures with 20% infill density were higher because the amount of material required to infill the structure was less, leading to the decreased tensile strength.

The range of tensile strength of the 3D printed samples with an infill density of 20%–100% was within 12 MPa–22 MPa. Although the tensile strength of the acoustic absorbers decreases with a decrease in infill densities, the range of tensile strength of the acoustic absorbers was much nearer or greater than the previously

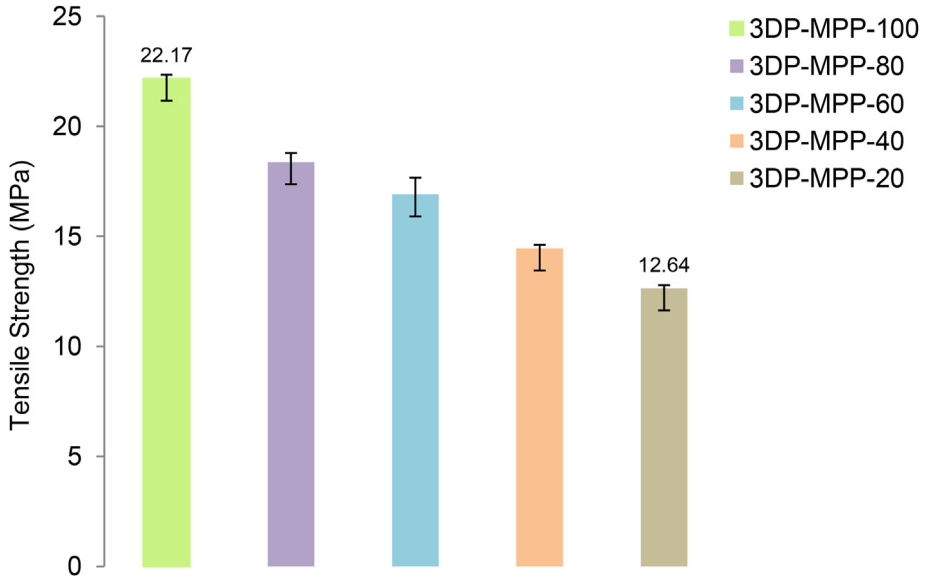

Fig. 8. Measured tensile strength of 3DP-MPP at varying infill densities.

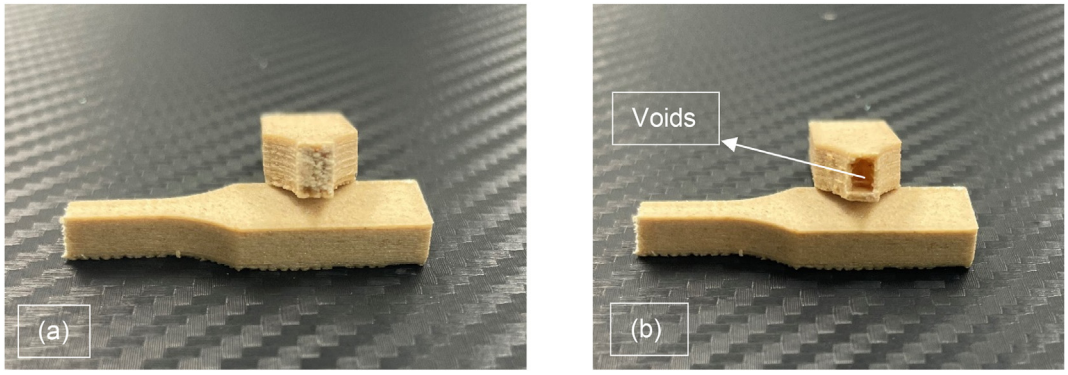

Fig. 9. Voids visible at fracture region after tensile testing. (a) 100% infill density, (b) 20% infill density.

reported acoustic absorbers such as fiber boards (12 MPa–27 MPa) [32], hardboards (26.30 MPa) [33], commercial ceiling board (23.5 MPa) [34] and ceiling boards (less than 2 MPa) [35,36].

5. Conclusions

Microperforated panels made of PLA/PHA-WF were successfully fabricated by additive manufacturing and its acoustic absorption was measured. The maximum sound absorption coefficient of the MPP with an infill density of 100% was 0.95 in the mid-frequency spectrum of 2000 Hz. Reducing the infill density decreases the mass of the MPP with the maximum of SAC for all the MPP with reduced infill densities around 0.9 at a resonant frequency within the same mid-frequency spectrum (2000 Hz–2600 Hz). The idea of reducing the mass of the MPP with maintaining the maximum SAC and without deviating its resonant frequency to other spectrums was demonstrated. The results obtained from increasing the air gap thickness demonstrated the shifting of resonant frequencies. Increasing the air gap thickness, shifts the peaks of acoustic absorption towards the lower frequency spectrum. MPP with an infill density of 100% at an air gap of 15 mm shows the maximum SAC of almost unity at 1100 Hz. The acoustic absorber fabricated with a 100% infill density has fewer voids in it since the amount of material used to infill was much higher compared to the sample 3D printed with a 20% infill density. This increased void content due to the reduced infill density has caused a drop in tensile strength of not less than 12 MPa. The proposed acoustic absorbers can be mounted on building walls or ceilings with an air gap for effective acoustic absorption.

Note on contributors

Vignesh Sekar is a research scholar from Taylor's University, Malaysia. His research interests include acoustic engineering, additive manufacturing, sound absorption of natural fiber composites, and material engineering.

Se Yong Eh Noum is a Programme Director - Bachelor of Robotic Design and Development (Honours), School of Computer Science and Engineering/Faculty of Innovation and Technology, Taylor's University, Malaysia. His area of expertise includes Material Sciences, Polymeric Materials and Polymer Composites.

Azma Putra is now an Associate Professor in Faculty of Mechanical Engineering, Universiti Teknikal Malaysia Melaka (UTeM). His research interests are in engineering acoustics and noise

control, structural dynamics and vibro-acoustics. Dr. Azma Putra is a member of Institute of Noise and Control Engineering (INCE), USA and Society of Vibration and Acoustics Malaysia (SVAM).

Sivakumar Sivanesan is a Head of School, School of Engineering, Asia Pacific University, Malaysia. His research area includes engineering education and material engineering.

Desmond Daniel Chin Vui Sheng is working as a lecturer in School of Mechanical Engineering, Faculty of Engineering, Universiti Teknologi Malaysia. His research interests include acoustic engineering, sound absorption of microperforated panel, sound absorption of natural fiber composites, sustainability engineering, material science, and manufacturing engineering.

Funding

This work was partially sponsored by Taylor's University Flagship Research Grant TUFR/2017/001/05.

Declaration of Competing Interest

The authors declare that they have no known competing financial interests or personal relationships that could have appeared to influence the work reported in this paper.

Acknowledgement

The author is thankful to the Taylor's University for funding scholarship during this research work. An acoustic impedance tube was used in collaboration with Universiti Teknikal Malaysia, Melaka.

References

[1] Z. Jafari, B.E. Kolb, M.H. Mohajerani, Chronic traffic noise stress accelerates brain impairment and cognitive decline in mice, Exp. Neurol. 308 (2018) 1–12, https://doi.org/10.1016/j.expneurol.2018.06.011.
[2] J. Ryu, H. Song, Y. Kim, Effect of the suspended ceiling with low-frequency resonant panel absorber on heavyweight floor impact sound in the building, Build. Environ. 139 (2018) 1–7, https://doi.org/10.1016/j.buildenv.2018.05.004.
[3] P. Newell, Recording Studio Design, Taylor & Francis US, 2008, https://doi.org/10.4324/9781315675367.
[4] N. Atalla, F. Sgard, Modeling of perforated plates and screens using rigid frame porous models, J. Sound Vib. 303 (1–2) (2007) 195–208, https://doi.org/10.1016/j.jsv.2007.01.012.
[5] C.M. Mak, Z. Wang, Recent advances in building acoustics: an overview of prediction methods and their applications, Build. Environ. 91 (2015) 118–126, https://doi.org/10.1016/j.buildenv.2015.03.017.
[6] M. Hosseini Fouladi, M.J.M. Nor, M. Ayub, Z.A. Leman, Utilization of coir fiber in multilayer acoustic absorption panel, Appl. Acoust. 71 (2010) 241–249, https://doi.org/10.1016/j.apacoust.2009.09.003.
[7] M. Dah-You, Theory and design of microperforated panel sound-absorbing constructions, Sci. Sin. 18 (1975) 55–71, https://doi.org/10.1360/YA1975-18-155.
[8] X. Gai, T. Xing, X. Li, B. Zhang, Z. Cai, F. Wang, Sound absorption properties of microperforated panel with membrane cell and mass blocks composite structure, Appl. Acoust. 137 (2018) 98–107, https://doi.org/10.1016/j.apacoust.2018.03.013.
[9] K. Sakagami, T. Nakamori, M. Morimoto, M. Yairi, Double-leaf microperforated panel space absorbers : a revised theory and detailed analysis, Appl. Acoust. 70 (2009) 703–709, https://doi.org/10.1016/j.apacoust.2008.09.004.
[10] K. Sakagami, M. Morimoto, M. Yairi, A note on the relationship between the sound absorption by microperforated panels and panel/membrane-type absorbers, Appl. Acoust. 70 (2009) 1131–1136, https://doi.org/10.1016/j.apacoust.2009.03.003.
[11] W. Guo, H. Min, A compound micro-perforated panel sound absorber with partitioned cavities of different depths, Energy Proc. 78 (2015) 1617–1622, https://doi.org/10.1016/j.egypro.2015.11.238.
[12] D. Daniel, C. Vui, Sound absorption of microperforated panel made from coconut fiber and polylactic acid composite, J. Nat. Fibers (2020) 1–11, https://doi.org/10.1080/15440478.2020.1821290.
[13] R. Lin, M. Toyoda, D. Takahashi, Sound insulation characteristics of multi-layer structures with a microperforated panel, Appl. Acoust. 72 (2011) 849–855, https://doi.org/10.1016/j.apacoust.2011.05.009.
[14] F. Asdrubali, G. Pispola, Properties of transparent sound-absorbing panels for use in noise barriers, J. Acoust. Soc. Am. 121 (1) (2007), https://doi.org/10.1121/1.2395916.
[15] U. Berardi, G. Iannace, Acoustic characterization of natural fibers for sound absorption applications, Build. Environ. 94 (2015) 840–852, https://doi.org/10.1016/j.buildenv.2015.05.029.
[16] H. Chen, L.D. Burns, Environmental analysis of textile products, Cloth. Text. Res. J. 24 (3) (2016) 248–261, https://doi.org/10.1177/0887302X06293065.
[17] V. Mazzanti, L. Malagutti, F. Mollica, FDM 3D printing of polymers containing natural fillers: a review of their mechanical properties, Polymers 11 (7) (2019) 1094, https://doi.org/10.3390/polym11071094.
[18] J. Smardzewski, T. Kamisi, D. Dziurka, A. Majewski, Sound absorption of wood-based materials, Holzforschung (April) (2015) 1–8, https://doi.org/10.1515/hf-2014-0114.
[19] F. Asdrubali, B. Ferracuti, L. Lombardi, C. Guattari, L. Evangelisti, G. Grazieschi, A review of structural, thermo-physical, acoustical, and environmental properties of wooden materials for building applications, Build. Environ. 114 (2017) 307–332, https://doi.org/10.1016/j.buildenv.2016.12.033.
[20] X.X. Tong, B. Hu, Review on research process of sound reduction materials review on research process of sound reduction materials, IOP Conf. Ser. Mater. Sci. Eng. 612 (2019), 052062, https://doi.org/10.1088/1757-899X/612/5/052062.
[21] V. Sekar, M.H. Fouladi, S.N. Namasivayam, S. Sivanesan, Additive manufacturing : a novel method for developing an acoustic panel made of natural fiber-reinforced composites with enhanced mechanical and acoustical properties, J. Eng. (2019) 19, https://doi.org/10.1155/2019/4546863. Article ID 4546863.
[22] V. Sekar, S.Y. Eh Noum, S. Sivanesan, A. Putra, D.D.C.V. Sheng, D.H. Kassim, Effect of thickness and infill density on acoustic performance of 3D printed panels made of natural fiber reinforced composites, J. Nat. Fibers (2021), https://doi.org/10.1080/15440478.2021.1944426.
[23] Z.A. Rachman, S. S Utami, J. Sarwono, R. Widyorini, H.R. Hapsar, The usage of natural materials for the green acoustic panels based on the coconut fibers and the citric acid solutions, IOP Conf. Series: J. Phys. Conf. 1075 (2018), 012048, https://doi.org/10.1088/1742-6596/1075/1/012048.
[24] I.B. Crandall, Theory of vibrating systems and sound, Nature 120 (1927) 544, https://doi.org/10.1038/120544b0.
[25] M.D. You, Theory of microslit absorbers, Chin. J. Acoust. 20 (2001) 1–10.
[26] Z. Liu, J. Zhan, M. Fard, J.L. Davy, Acoustic properties of multilayer sound absorbers with a 3D printed micro-perforated panel, Appl. Acoust. 121 (2017) 25–32, https://doi.org/10.1016/j.apacoust.2017.01.032.
[27] International Organization for Standardization, ISO 10534-2, Acoustics-Determination of Sound Absorption Coefficient and Impedance in Impedance Tubes, Int. Stand., 2001.
[28] K. V Horoshenkov, A. Khan, F. Bécot, L. Jaouen, F. Sgard, F. Pompoli, N. Prodi, P. Bonfiglio, G. Pispola, F. Asdrubali, Reproducibility experiments on measuring acoustical properties of rigid-frame porous media (round-robin tests), J. Acoust. Soc. Am. 122 (2007) 345–354, https://doi.org/10.1121/1.2739806.
[29] K.M. Ho, Z. Yang, X.X. Zhang, P. Sheng, Measurements of sound transmission through panels of locally resonant materials between impedance tubes, Appl. Acoust. 66 (2005) 751–765, https://doi.org/10.1016/j.apacoust.2004.11.005.
[30] D. Daniel, V. Sheng, M. Nizam, B. Yahya, N. Bin, C. Din, P. Ong, Acoustic properties of biodegradable composite micro-perforated panel (BC-MPP) made from kenaf fi bre and polylactic acid (PLA), Appl. Acoust. 138 (2018) 179–187, https://doi.org/10.1016/j.apacoust.2018.04.009.
[31] V. Sekar, S.Y. Eh Noum, A. Putra, S. Sivanesan, K.C. Chin, Y.S. Wong, D.H. Kassim, Acoustic properties of micro-perforated panels made from oil palm empty fruit bunch fiber reinforced polylactic acid, Sound Vib. 55 (4) (2021) 343–352, https://doi.org/10.32604/sv.2021.014916.
[32] N. Narlıoğlu, T. Salan, N.S. Cetin, M.H. Alma, Evaluation of furniture industry wastes in polymer composite production, Furniture and Wooden Material Research Journal 1 (2) (2018) 78–85, https://doi.org/10.33725/mamad.492418.
[33] J.F. Hunt, C.B. Vick, Strength and processing properties of wet-formed hardboards from recycled corrugated containers and commercial hardboard fibers, For. Prod. J. 49 (5) (1999) 69–74.
[34] V.I.E. Ajiwe, C.A. Okeke, S.C. Ekwuozor, I.C. Uba, Pilot plant for production of ceiling boards from rice husks, Bioresour. Technol. 66 (1) (1998) 41–43, https://doi.org/10.1016/S0960-8524(98)00023-6.
[35] A.A. Adediran, O.A. Balogun, A.A. Akinwande, O.S. Adesina, O.S. Olasoju, Influence of chemical treatment on the properties of cement-paper hybrid composites for ceiling board application, Heliyon 6 (2020), e04512, https://doi.org/10.1016/j.heliyon.2020.e04512.
[36] I.O. Ohijeagbon, M.U. Bello-Ochende, A.A. Adeleke, P.P. Ikubanni, A.A. Samuel, O.A. Lasode, O.D. Atoyebi, Physico-mechanical properties of cement bonded ceiling board developed from teak and African locust bean tree wood residue, Mater. Today Proc. 44 (2021) 2865–2873, https://doi.org/10.1016/j.matpr.2020.12.1170.